View metadata, citation and similar papers at core.ac.uk

brought to you by CORE

provided by Purdue E-Pubs

Purdue University
Purdue e-Pubs

International Refrigeration and Air Conditioning Conference

School of Mechanical Engineering

2016

Modeling of Finned-Tube Heat Exchangers: A Novel Approach to the Analysis of Heat and Mass Transfer under Cooling and Dehumidifying Conditions

Hongtao Qiao
Mitsubishi Electric Research Laboratories, United States of America, qiao@merl.com

Christopher R. Laughman
Mitsubishi Electric Research Laboratories, United States of America, laughman@merl.com

Follow this and additional works at: http://docs.lib.purdue.edu/iracc

Qiao, Hongtao and Laughman, Christopher R., "Modeling of Finned-Tube Heat Exchangers: A Novel Approach to the Analysis of Heat and Mass Transfer under Cooling and Dehumidifying Conditions" (2016). *International Refrigeration and Air Conditioning Conference*. Paper 1699.
http://docs.lib.purdue.edu/iracc/1699

This document has been made available through Purdue e-Pubs, a service of the Purdue University Libraries. Please contact epubs@purdue.edu for additional information.
Complete proceedings may be acquired in print and on CD-ROM directly from the Ray W. Herrick Laboratories at https://engineering.purdue.edu/Herrick/Events/orderlit.html

Modeling of Finned-Tube Heat Exchangers: A Novel Approach to the Analysis of Heat and Mass Transfer under Cooling and Dehumidifying Conditions

Hongtao QIAO*, Christopher R. LAUGHMAN

Mitsubishi Electric Research Laboratories
Cambridge, MA 02139
{qiao, laughman}@merl.com

ABSTRACT

The construction of physics-based models of the simultaneous heat and mass transfer on the air-side surface of air-cooled fin-and-tube heat exchangers during dehumidification can present distinct challenges. Because only part of the external surface of a finite length finned tube may be wetted in the radial and/or axial directions, the determination of the wet/dry boundary for this partially wet tube surface must parsimoniously describe the nonlinear variations in both the refrigerant temperature and air temperature profiles. A literature review indicates that extant heat exchanger models tend not to consider the partially wet conditions due to modeling complexity; moreover, many standard dehumidification models in the literature also exhibit significant deficiencies. For instance, the Lewis number is often incorrectly assumed to be unity, and the air saturation enthalpy at the surface interface is also assumed to be a linear function of temperature in both the Effectiveness model and the LMED (Logarithmic-Mean Enthalpy Difference) model. These simplifying assumptions can often introduce appreciable deviations between simulation outputs and measured data.

This paper proposes a new heat exchanger model that aims to address these challenges through new modeling approaches. After reviewing extant heat exchanger models that include the effects of dehumidification, a novel approach based upon the underlying physics is presented to analyze the air-side simultaneous heat and mass transfer. This new approach has a number of distinct advantages, including the fact that it allows scenarios with non-unity values of the Lewis number to be modeled, as well as the fact that the model accuracy is also significantly improved over extant models because of the assumption of the air saturation humidity ratio as a cubic function of temperature. In addition, these models allow the dry-wet boundary for partially wet surfaces to be readily determined from both air flow and refrigerant flow directions. A tube-by-tube analysis (which can be easily extended to a segment-by-segment analysis) including multiple refrigerant phases is adopted to allow for the simulation of complex tube circuitries. Results from this new approach are validated with experimental data reported in literature, and demonstrate good agreement.

1. INTRODUCTION

Finned-tube heat exchangers, made of aluminum, copper, steel and other materials, are the major components for heat transfer between air and fluids in the HVAC&R systems, and play a vital role in the manufacturing cost and system performance. The design of plate-fin-tube heat exchangers is a rather complex process in which a number of design aspects, including geometrical and operational parameters, tube and fin surfaces, coil configuration and refrigerant circuitry configuration, etc., are determined to satisfy specified requirements such as outlet temperature, heat duty and pressure drop. Due to a large number of design variables and a wide variety of factors that need to be taken into consideration, the traditional trial-and-error based engineering practice is time-consuming, and the design obtained may not be the optimal design with the best performance at the lowest cost. Therefore, an approach using the model-based design and optimization is attractive in order to reduce the guesswork at the design process and at the same time to yield a cost-optimal solution.

Detailed modeling for the finned-tube heat exchangers may be quite involved due to the complexity of coil geometry as well as multi-phase flow and heat transfer phenomena. However, the development of a detailed and fundamentally justified model is appealing and worthwhile because more accurate model predictions can be obtained. Although computationally expensive, a rigorous tube-by-tube or segment-by-segment analysis is often adopted for an accurate performance evaluation for this type of heat exchangers, i.e., the performance of each tube in the heat exchanger is analyzed separately and each tube is associated with different refrigerant parameters and air mass flow rate, inlet temperature and humidity, since they allow for the analysis of complex tube circuitries and air flow propagation as well as air/refrigerant flow maldistribution. In tube-by-tube models (Domanski and Didion

1983; Lee and Domanski, 1997), each tube is defined as a calculation domain. In segment-by-segment models (Liang et al., 2001; Jiang et al., 2006), each tube is further divided into several small segments each of which is a calculation domain. The calculation procedure of the segment-by-segment method is essentially the same as that of the tube-by-tube method except that the former takes advantage of the refined discretization and is capable of accounting for two-dimensional air flow maldistribution and significant changes in local refrigerant/air properties and heat transfer coefficients along the tube length.

One of the major challenges to evaluate the performance of the finned-tube heat exchangers is the analysis of the simultaneous heat and mass transfer characteristics on the coil surface during a dehumidifying process. Depending upon the operating conditions, the coil surface may be fully dry, fully wet or partially wet. If the fin base surface temperature is higher than the dew point of the air stream, only sensible heat transfer occurs, resulting in a fully dry fin. If the fin tip temperature is lower than the dew point of the air stream, simultaneous heat and mass transfer occurs, resulting in a fully wet fin. If the fin base temperature is lower but fin tip temperature is higher than the dew point of the air stream, only a part of fin surface is wet, referred as partially wet surface condition. Although seemingly complicated, the crucial point to evaluating the heat transfer performance on partially wet surface is quite straightforward, i.e., partitioning the dry and wet surfaces. Given the conditions that have to be satisfied at the point separating the wet and dry surfaces, i.e., the surface temperature is equal to the dew point of the air and the heat flow should be continuous, the dry-wet surface boundary can be mathematically determined although numerical iterations might be involved. Once the dry-wet surface boundary is obtained, the performance of dry and wet surfaces can be separately evaluated using the fully dry and fully wet methods. These principles actually prevail in a series of papers on the analysis of heat transfer for fully and partially wet fin assembly (El-Din, 1998; Rosario and Rahman, 1999).

Through scrutiny of these interesting and note-worthy papers, it can be found that all the analyses were based on a prevailing assumption, i.e., the air flow is static and the temperature of the air is uniform over the entire surface. However, this assumption can result in significant discrepancies if the approaches in these papers are used to predict the performance of the finned-tube heat exchanger under dehumidifying conditions since air state parameters, including temperature and humidity ratio, vary while air stream flows through the passages between the fins and tubes. In general, for a finite-length finned tube segment, it is possible that only a part of the outside surface is wetted in either the radial direction or axial direction or in both directions. Moreover, the shape of the dry-wet surface boundary in the radial direction will be extremely irregular and will no longer remain straight for rectangular fins or circular for radial fins. As a result, extant finned-tube heat exchanger models tend not to consider the partially wet conditions due to modeling complexity. Instead, in these models each calculation domain is assumed to be either completely dry or wet, based on the mean tube/fin surface temperature. However, neglecting the partially wet surface condition can lead to fundamental errors in the performance analysis of heat exchangers. Therefore, a new approach that can effectively address this challenge needs to be developed.

When it comes to the analysis of simultaneous heat and mass transfer between water-wetted surfaces and air, enthalpy difference based methods, e.g., LMED method (Threlkeld, 1970) and Effectiveness method (Braun et al., 1989), are often used, i.e., the driving potential for simultaneous heat and mass transfer is, to a close approximation, enthalpy. However, the use of these methods requires the assumptions that the Lewis number is unity and the enthalpy of the saturated air at the surface interface is a linear function of temperature. Inevitably, these assumptions can introduce appreciable deviations between simulation outputs and measured data under the conditions where the Lewis number actually deviates from unity and a wide range of operating temperatures exists. Consequently, an effective approach that does not rely on these assumptions is needed.

To address the challenges and problems identified above, the presented study intends to develop a new model to evaluate the thermal performance for finned-tube heat exchangers under cooling and dehumidifying conditions. The remainder of the paper is organized as follows. Section 2 presents the analysis for simultaneous heat and mass transfer between water-wetted surface and moist air. Section 3 describes the details for the proposed finned-tube heat exchanger model. Model validation is then discussed in Section 4. The final section concludes the paper with conclusions.

2. ANALYSIS FOR SIMULTANEOUS HEAT AND MASS TRANSFER

Fig. 1 shows schematically a cold surface in contact with a moving stream of moist air. Immediately next to the cold surface, the air is assumed to be saturated at the surface temperature. For the differential surface area in Fig .1, the simultaneous heat and mass transfer between the wetted surface and air is governed by the following equations

$$-\dot{m}_a dh = dQ - \dot{m}_a h_{f,w} d\omega \tag{1}$$

$$dQ = \alpha_c \left(T - T_w\right) dA_o + \alpha_m \left(\omega - \omega_{s,w}\right)\left(h_{g,t} - h_{f,w}\right) dA_o \tag{2}$$

$$-\dot{m}_a d\omega = \alpha_m \left(\omega - \omega_{s,w}\right) dA_o \tag{3}$$

Using the Lewis analogy $Le^{2/3} = \alpha_c/(\alpha_m c_{p,a})$ and recognizing $c_{p,a}(T - T_w) \approx (h - h_{s,w}) - (\omega - \omega_{s,w})$, Eq. (2) can be rewritten as

$$dQ = \frac{\alpha_c dA_o}{c_{p,a}}\left[\left(h - h_{s,w}\right) + \left(\omega - \omega_{s,w}\right)\left(\frac{h_{g,t} - h_{f,w}}{Le^{2/3}\Delta h_{fg}} - 1\right)\Delta h_{fg}\right] \tag{4}$$

where $h_{g,t}$ is the specific enthalpy of saturated water vapor at the air temperature T, $h_{f,w}$ is the specific enthalpy of liquid water at the wall temperature T_w, Δh_{fg} is the vaporization heat of water at 0°C (2501 kJ/kg). In Eq.(4), the Lewis number is often assumed to be unity, and the second group in the brackets is neglected since it is small compared to the term $(h - h_{s,w})$ (Threlkeld, 1970). Thus, the following expression can be obtained

$$dQ = \frac{\alpha_c dA_o}{c_{p,a}}\left(h - h_{s,w}\right) \tag{5}$$

Eq. (5) is the basis for the enthalpy difference methods. To simplify the analysis, many extant models (Threlkeld, 1970; Braun et al., 1989) used a linearization between air saturation enthalpy between temperature, i.e., $h_s = a + bT_s$, where a and b are the coefficients for the linearization. However, this simplification is only valid over a narrow range of temperature and can introduce appreciable errors when a wide range of the operating temperatures exists. Fig. 2 shows the variations in air saturation enthalpy and its derivative with respect to temperature. Clearly, air saturation enthalpy does not vary linearly with temperature, and its derivative changes significantly with temperature. In light of it, a new approach free of these restrictions is proposed.

The analysis is started by substituting Eq. (2) and (3) into (1), yielding

$$-\dot{m}_a dh = \alpha_c dA_o \left(T - T_w\right) + \alpha_m dA_o \left(\omega - \omega_{s,w}\right)\left(h_{g,t} - h_{f,w}\right) + \alpha_m dA_o \left(\omega - \omega_{s,w}\right) h_{f,w} \tag{6}$$

Eq. (6) can be rearranged as

$$\alpha_c dA_o \left(T - T_w\right) = \dot{m}_a \left(-dh + h_{g,t} d\omega\right) \tag{7}$$

Differentiating $h = c_{p,a}T + \Delta h_{fg}\omega$ yields

$$dh = d\left(c_{p,a}T\right) + \Delta h_{fg} d\omega = c_{p,a} dT + T dc_{p,a} + \Delta h_{fg} d\omega \tag{8}$$

Substituting Eq. (8) into the right hand side of Eq.(7) gets

$$\dot{m}_a \left(-dh + h_{g,t} d\omega\right) = \dot{m}_a \left(-c_{p,a} dT - T dc_{p,a} - \Delta h_{fg} d\omega + h_{g,t} d\omega\right) = \dot{m}_a \left[-c_{p,a} dT + \left(h_{g,t} - \Delta h_{fg}\right) d\omega - T dc_{p,a}\right] \tag{9}$$

The specific enthalpy of saturated water vapor at the dry-bulb temperature $h_{g,t}$, is given by

$$h_{g,t} = c_{p,g,H_2O} T + \Delta h_{fg} \tag{10}$$

where $c_{p,g,H2O}$ is the specific heat of water vapor (≈1.805 kJ/kg) and the vaporization heat of water at 0°C, Δh_{fg}, is 2501 kJ/kg. Specific heat of moist air $c_{p,a}$ is determined as

$$c_{p,a} = c_{p,da} + c_{p,g,H_2O}\omega \tag{11}$$

where $c_{p,da}$ is the specific heat of dry air (≈1.006 kJ/kg). Therefore

$$\left(h_{g,t} - \Delta h_{fg}\right) d\omega - t dc_{p,a} = c_{p,g,H_2O} T d\omega - c_{p,g,H_2O} T d\omega = 0 \tag{12}$$

Eventually, Eq. (7) can be simplified as

$$\alpha_c dA_o \left(T - T_w\right) = -\dot{m}_a c_{p,a} dT \tag{13}$$

Eq. (13) indicates that the temperature change of the air stream under cooling and dehumidification conditions is completely determined by the sensible heat transfer between the wetted surfaces and the air, driven by the temperature difference. On the other hand, Eq. (3) indicates that the change in the humidity ratio of air stream is completely determined by the mass transfer between the bulk of air stream and the air immediately adjacent to the wetted surfaces, driven by the difference in water vapor concentration.

Therefore, Eq. (13) can be used in place of Eq. (1) to calculate the sensible heat transfer; Eq. (2) can be used to calculate the overall heat transfer; Eq. (3) can be used to calculate the mass transfer. In order to simplify the analysis, a cubic approximation is used to determine the saturation humidity ratio as a function of temperature, i.e.

$$\omega_s = \kappa_3 T^3 + \kappa_2 T^2 + \kappa_1 T + \kappa_0 \tag{14}$$

As shown in Fig. 3, this cubic approximation can fit the data much better over a wide range of temperatures, e.g., 0°C ~ 40°C, than a linear approximation. More importantly, significant model simplification can be achieved with this approximation, as will be shown shortly (note: model simplification can be also achieved with linear or quadratic approximation, but with lower precision).

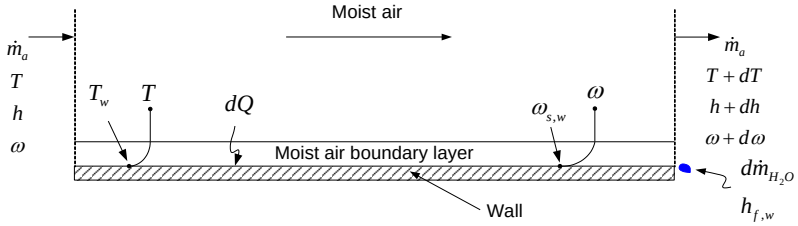

Fig. 1 Cooling and dehumidifying of moist air

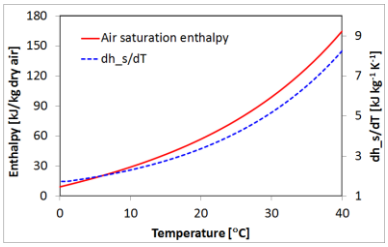

Fig. 2 Air saturation saturation and its derivative

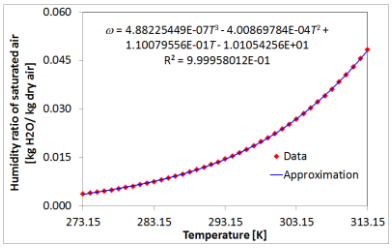

Fig. 3 Cubic approximation of saturation humidity ratio

3. MODELING APPROACH

The presented heat exchanger model is based on the tube-by-tube approach, i.e., the performance of each tube, associated with different refrigerant and air parameters, is evaluated separately. Simulation starts with the refrigerant inlet tube of a given circuit and progresses consecutively to the following tubes until the outlet is reached. When the surface temperature is below the dew point of the air, simultaneous heat and mass transfer occurs on the external surfaces of the heat exchanger, resulting in removal of water vapor from the air stream by condensation. The condensate will flow down the tubes and fins due to the gravity effect. It must be pointed out that water vapor can sublimate directly into the solid state (i.e., frost) when the surface temperature is lower than the freezing point. In this paper, however, the frost phenomenon will not be discussed due to the space constraint.

3.1 Fully Dry Tube

When all the surface temperatures are above the dew point of the air stream, only sensible heat transfer occurs on the air side. In this case, heat transport between the refrigerant and the air is driven by the temperature difference, and water vapor in the moist air still stays in the gaseous phase and does not condense to liquid water. The heat that the air rejects to the refrigerant results in the decline in air temperature. The heat transfer process between the air and refrigerant in a cross flow configuration with one tube, as shown in Fig. 4, can be mathematically described by Eqs. (15) and (16).

$$\dot{m}_a \frac{dx}{L_x} c_{p,a} dT_a = -U_o \left(T_a - T_r\right) dA_o \tag{15}$$

$$\dot{m}_r dh_r = -\dot{m}_a \frac{dx}{L_x}\left[T_a\left(x, L_y\right) - T_a\left(x, 0\right)\right] \tag{16}$$

where U_o is the overall heat transfer coefficient based on the total external surface area defined as $U_o = 1/(R_{ad} + R_{md} + \phi R_r)$. Various thermal resistances can be calculated based on ARI Standard 410 (2001). ϕ is the ratio of total external coil surface area to the total internal surface area, A_o/A_i. $dA_o = A_o(dx/L_x)(dy/L_y)$.

It is assumed that refrigerant temperature varies only in the *x* direction and air temperature varies in both the *x* and *y* directions since the fins prevent mixing in a plane normal to the flow. Assuming air inlet temperature is uniform along the tube length, single-phase refrigerant temperature distribution can be obtained by integrating Eqs. (15) and (16).

$$T_r(x) = T_{a,1} + (T_{r,1} - T_{a,1}) \exp\left\{ -\frac{\dot{m}_a c_{p,a}}{\dot{m}_r c_{p,r}} \left[1 - \exp(-NTU)\right] \frac{x}{L_x} \right\} \tag{17}$$

where *NTU* is the number of transfer units defined as $NTU = U_o A_o / (\dot{m}_a c_{p,a})$.

The two-dimensional air temperature distribution is

$$T_a(x,y) = T_r(x) - \left[T_r(x) - T_{a,1}\right] \exp\left(-NTU \frac{y}{L_y} \right) \tag{18}$$

The external surface temperature is

$$T_w(x,y) = \frac{(R_{mD} + \phi R_r) T_a(x,y) + R_{aD} T_r(x)}{R_{aD} + R_{mD} + \phi R_r} \tag{19}$$

With Eq. (17) it is easy to compute the average temperature of the air stream leaving the tube

$$\bar{T}_{a,2} = \frac{1}{L_x} \int_{x=0}^{x=L_x} T_a(x, L_y) dx = \frac{\dot{m}_r (h_{r,2} - h_{r,1})}{\dot{m}_a c_{p,a}} + T_{a,1} \tag{20}$$

In two-phase, refrigerant temperature is dependent upon both pressure and quality. To avoid complex analyses involving numerical integration, it is assumed that refrigerant temperature varies linearly along the tube length, i.e.

$$T_r(x) = T_{r,1} + \int_0^x \frac{dT_r}{dz} dz \approx T_{r,1} + \frac{T_{r,2} - T_{r,1}}{L_x} x \tag{21}$$

Substituting Eq. (21) into Eq. (15) and integrating yields

$$Q = \frac{\dot{m}_a c_{p,a}}{L_x} \int_{x=0}^{x=L_x} \left[1 - \exp(-NTU)\right] \left[T_{a,1} - \left(T_{r,1} + \int_0^x \frac{dT_r}{dz} dz \right) \right] dx \approx \dot{m}_a c_{p,a} \left[1 - \exp(-NTU)\right] \left(T_{a,1} - \frac{T_{r,1} + T_{r,2}}{2} \right) \tag{22}$$

The enthalpy of refrigerant leaving the tube can be iteratively computed since $T_{r,2} = T(p_2, h_2)$ is based on the energy balance $Q = \dot{m}_r (h_{r,2} - h_{r,1})$.

3.2 Fully Wet Tube

Depending upon operating conditions, the coil can operate in completely wet condition. In this case, all the surface temperatures are below the dew point of the air stream. Eqs. (23) - (27) are used to describe the simultaneous heat and mass transfer between moist air and refrigerant.

$$\frac{T_w - T_r}{R_{mW} + \phi R_r} = \frac{(T_a - T_w)}{R_{aW}} + \alpha_m (\omega_a - \omega_w) (h_{ga,H_2O} - h_{f,H_2O}) \tag{23}$$

$$\frac{T_w - T_r}{R_{mW} + \phi R_r} dA_o = -\frac{\dot{m}_a}{L_x} (dh_a - h_{f,H_2O} d\omega) \tag{24}$$

$$\dot{m}_r dh_r = -\frac{\dot{m}_a}{L_x} \left[h_a(x, L_y) - h_a(x,0) - \int_{y=0}^{y=L_y} h_{f,H_2O} d\omega \right] \tag{25}$$

$$d\dot{m}_{H_2O} = -\frac{\dot{m}_a}{L_x} d\omega \tag{26}$$

$$d\dot{m}_{H_2O} = \alpha_m (\omega_a - \omega_w) dA_o \tag{27}$$

These equations have no closed-form solution, and need to be discretized along both *x* and *y* directions and solved numerically. Obviously, rigorous discretization is computationally expensive although it allows for an accurate

analysis. To improve the numerical efficiency, a simplified approach is developed in which the average state of the air leaving the tube is approximated by averaging the state of the air leaving both ends (inlet and outlet) of the tube.

$$\begin{aligned}\bar{T}_{a,2} &= \frac{1}{L_x}\int_{x=0}^{x=L_x} T_a\left(x, L_y\right)dx \approx \left[T_a\left(0, L_y\right) + T_a\left(L_x, L_y\right)\right]/2 \\ \bar{\omega}_{a,2} &= \frac{1}{L_x}\int_{x=0}^{x=L_x} \omega_a\left(x, L_y\right)dx \approx \left[\omega_a\left(0, L_y\right) + \omega_a\left(L_x, L_y\right)\right]/2\end{aligned} \tag{28}$$

Then the problem becomes how to compute air states at the positions (0, L_y) and (L_x, L_y). During the process of heat and mass transport, the state of the air changes continuously along its flow pathway. Therefore, discretization along the air flow pathway, i.e., the *y* direction, must be applied to obtain a reasonably accurate evaluation of the variations in air states. The analysis starts with dividing the tube into *n* sections equally along the *y* direction, as shown in Fig. 5. At the inlet end of the tube, there are *n* positions (the red points in Fig. 5) where the air state needs to be computed (remember that the air state at the first red point is known as the boundary conditions). The following equations should hold at for the (i-1)th section

$$\frac{T_{w,i} - T_r}{R_{mW} + \phi R_r} = \frac{T_{a,i} - T_{w,i}}{R_{aW}} + \alpha_m\left(\omega_{a,i} - \omega_{w,i}\right)\Delta h_{fg,i} \tag{29}$$

$$\frac{\dot{m}_a c_{p,a}}{\Delta A}\left(T_{a,i-1} - T_{a,i}\right) = \frac{1}{R_{aW}}\left(\frac{T_{a,i-1} + T_{a,i}}{2} - \frac{T_{w,i-1} + T_{w,i}}{2}\right) \tag{30}$$

$$\frac{\dot{m}_a}{\Delta A}\left(\omega_{a,i-1} - \omega_{a,i}\right) = \alpha_m\left(\frac{\omega_{a,i-1} + \omega_{a,i}}{2} - \frac{\omega_{w,i-1} + \omega_{w,i}}{2}\right) \tag{31}$$

where T_r is the local refrigerant temperature and $\Delta A = A_o/n$. Eq. (29) is the heat transfer equation between the air and the refrigerant, whereas Eqs. (30) and (31) are the equations that compute the changes in air temperature and humidity ratio (please refer to Section 2), respectively. These equations can be derived by using the center difference and assuming that refrigerant temperature T_r does not vary along the entire tube. Since they are written in the form of heat flux, these equations actually hold at any position as long as the *y* coordinate of that position is the same as that of the point *i*. Solving Eqs. (29)- (31) yields a cubic equation of $T_{w,i}$, i.e.

$$aT_{w,i}^3 + bT_{w,i}^2 + cT_{w,i} + d = 0 \tag{32}$$

Solving $T_{w,i}$ via Eq. (32) and substituting it into Eq. (30), $T_{a,i}$ can be obtained. $\omega_{a,i}$ can be calculated from Eq. (14). As a result, air states can be recursively computed until the state of the air leaving the inlet end (at point *n*) is obtained. To close this recursive loop, however, the coil surface temperature at the first point (point 0) is required. It can be determined by iterating Eq. (29) since the enthalpy of the condensate $h_{f,H2O}$ needs to be evaluated at this temperature. Please note that there is no need to evaluate $\Delta h_{fg,H2O}$ at every local point. To further simplify the analysis, $\Delta h_{fg,H2O}$ at the first point can be used throughout without introducing noticeable deviations. The above analysis is repeated to solve for the state of the air leaving the outlet end of the tube. A grid independency study has been conducted, showing that only four sections (n = 4) are necessary to discretize the tube along the y direction and more sections result in negligible changes in the results.

3.3 Partially Wet Tube

Depending upon operating conditions, there are nine possible coil surface conditions, as shown in Fig. 6. In the figure, the refrigerant flows from the left to the right and the air flows upward; the shaded area denotes the wetted surface and the unshaded area denotes the dry surface. The cases where all surfaces are completely wet and dry have been discussed in Section 3.1 and 3.2, respectively. In the remaining cases, a part of the coil is dry with the surface temperatures above the entering air dew-point temperature, whereas the remainder of the coil is wet with the surface temperatures below the entering air dew-point temperature. For these cases, the performance of the dry and wet portions of the coil should be evaluated separately. Therefore, it is crucial to determine the boundary between the dry surface and wet surface regions. Since the coil surface temperatures are equal to the entering air dew point temperature on the dry-wet boundary, one can equate the external coil surface temperatures calculated by Eq. (19) with the entering air dew point temperature, yielding

$$T_{a,dp}=\frac{\left(R_{mD}+\phi R_r\right)T_a\left(x,y\right)+R_{aD}T_r\left(x\right)}{R_{aD}+R_{mD}+\phi R_r}\Rightarrow f_{y,wo}\left(x\right)=\frac{y_{wo}\left(x\right)}{L_y}=\frac{1}{NTU}\ln\left[\frac{R_{mD}+\phi R_r}{R_{aD}+R_{mD}+\phi R_r}\cdot\frac{T_{a,1}-T_r\left(x\right)}{T_{a,dp}-T_r\left(x\right)}\right] \tag{33}$$

where $f_{y,wo}$ is the relative position of the local onset location of the wet surface along the y direction. If the refrigerant temperature profile $T_r(x)$ is known, Eq. (33) can actually determine the two-dimensional boundary between the dry and wet surface regions. However, it is impossible to obtain the analytical solution of $T_r(x)$ in wet conditions. Instead, Eq. (33) will be used to determine to which case depicted in Fig. 6 the actual coil surface condition belongs, and then the fraction of the tube length for the fully wet region, partially wet region and fully dry region will be computed. Heat transfer performance of each region will be evaluated separately and add up to obtain the overall performance of the entire tube. As a result, Eq. (33) needs to be evaluated for both ends of the tube. Negative values for $f_{y,wo}(x)$ mean that the dehumidification occurs even before the air reaches the tube, denoting that the surface is fully wet. Values larger than unity for $f_{y,wo}(x)$ mean the dehumidification occurs after the air leaves the tube, denoting that the surface is fully dry. Values between zero and unity for $f_{y,wo}(x)$ mean the dehumidification occurs somewhere on the coil surface along the air flow path, denoting that the surface is partially wet. Specifically, the following criteria are used to determine the cases depicted in Fig. 6.

Case (a): $f_{y,wo}(x = 0) \le 0$ && $f_{y,wo}(x = L_x) \le 0$; Case (b): $f_{y,wo}(x = 0) \le 0$ && $0 < f_{y,wo}(x = L_x) \le 1$; Case (c): $f_{y,wo}(x = 0) \le 0$ && $f_{y,wo}(x = L_x) > 1$; Case (d): $0 < f_{y,wo}(x = 0) < 1$ && $f_{y,wo}(x = L_x) \le 0$; Case (e): $0 < f_{y,wo}(x = 0) < 1$ && $0 < f_{y,wo}(x = L_x) \le 1$; Case (f): $0 < f_{y,wo}(x = 0) < 1$ && $f_{y,wo}(x = L_x) > 1$; Case (g): $f_{y,wo}(x = 0) \ge 1$ && $f_{y,wo}(x = L_x) \le 0$; Case (h): $f_{y,wo}(x = 0) \ge 1$ && $0 < f_{y,wo}(x = L_x) \le 1$; Case (i): $f_{y,wo}(x = 0) \ge 1$ && $f_{y,wo}(x = L_x) > 1$.

Without loss of generality, Case (b) and (c) will be discussed to illustrate how to evaluate the heat transfer performance of a tube that has both dry and wet surface regions (Fig. 7).

For the Case (b), the onset location of the wet surface at the inlet and outlet of the tube satisfies $f_{y,wo}(x = 0) \le 0$ && $0 < f_{y,wo}(x = L_x) \le 1$. In this case, there is no fully dry surface, i.e., $f_{x,fd} = 0$. The average state of the air leaving the tube is approximately determined by the length-weighted state of the fully and partially wet surface regions, i.e.

$$\begin{aligned}\bar{T}_{a,2}&=\frac{1}{L_x}\int_{x=0}^{x=L_x}T_a\left(x,L_y\right)dx\approx\frac{f_{x,fw}T_a\left(0,L_y\right)}{2}+\frac{\left(f_{x,fw}+f_{x,pw}\right)T_a\left(f_{x,fw}L_x,L_y\right)}{2}+\frac{f_{x,pw}T_a\left(L_x,L_y\right)}{2}\\ \bar{\omega}_{a,2}&=\frac{1}{L_x}\int_{x=0}^{x=L_x}\omega_a\left(x,L_y\right)dx\approx\frac{f_{x,fw}\omega_a\left(0,L_y\right)}{2}+\frac{\left(f_{x,fw}+f_{x,pw}\right)\omega_a\left(f_{x,fw}L_x,L_y\right)}{2}+\frac{f_{x,pw}\omega_a\left(L_x,L_y\right)}{2}\end{aligned} \tag{34}$$

The state of the air at (0, L_y) and ($f_{x,fw}L_x$, L_y) can be computed using the discretized approach introduced in Section 3.2 since the air flow pathways passing these two individual locations are fully wetted. The local refrigerant temperature at $x = f_{x,fw}L_x$ can be readily computed via Eq. (33) by imposing the condition $f_{y,ow}(x = f_{x,fw}L_x) = 0$. The state of the air at (L_x, L_y) should be computed differently since only a part of the air flow pathway at the outlet end of the tube is wetted. Along this air flow pathway, air temperature and coil surface temperature at the dry-wet transition point can be determined by Eq. (18) and (19) by substituting $x = L_x$ and $y = y_{ow}(x = L_x)$, respectively. Similarly, the remaining wetted air flow pathway can be solved using the discretized method. The only difference is that the boundary conditions are the computed air temperature and coil surface temperature at the dry-wet transition point, and the distance of the air flow pathway is $L_y - y_{ow}(x = L_x)$.

However, the fraction of the fully wet surface region $f_{x,fw}$ still needs to be determined. The pertinent steps are described as follows:

(1) Guess the fraction of the fully wetted region $f_{x,fw}$.

(2) Compute the heat transfer rate for the fully wet surface region

$$Q_{fw}=f_{x,fw}\left[\dot{m}_a\bar{c}_{p,a}\left(T_{a,1}-\bar{T}_{a,fw}\right)+\dot{m}_a\Delta h_{fg}\left(\omega_{a,1}-\bar{\omega}_{a,fw}\right)\right] \tag{35}$$

where $\bar{T}_{a,fw}=\left[T_a\left(0,L_y\right)+T_a\left(f_{x,fw}L_x,L_y\right)\right]/2$, $\bar{\omega}_{a,fw}=\left[\omega_a\left(0,L_y\right)+\omega_a\left(f_{x,fw}L_x,L_y\right)\right]/2$.

(3) Based on the energy balance, refrigerant enthalpy at $x = f_{x,fw}L_x$ is determined as $h_r\left(x=f_{x,fw}L_x\right)=h_{r,1}+Q_{fw}/\dot{m}_r$.

(4) The local refrigerant temperature at $x = f_{x,fw}L_x$ can be evaluated using the information of the computed pressure and enthalpy.
(5) Check if the computed refrigerant temperature at $x = f_{x,fw}L_x$ in (4) is equal to the value obtained via Eq. (33). If yes, $f_{x,fw}$ is the solution. If not, iterate $f_{x,fw}$ and go back to (2) until convergence is obtained.

Alternatively, the fraction of the fully wet surface region can be approximately computed without any iteration. Assuming that refrigerant temperature varies linearly along the tube length in two-phase, $f_{x,fw}$ can be directly solved via $f_{x,fw} = \left[T_r\left(x = f_{x,fw}\right) - T_{r,1}\right] / \left(T_{r,2} - T_{r,1}\right)$ given the local refrigerant temperature at $x = f_{x,fw}L_x$ computed via Eq. (33). In single-phase, $f_{x,fw}$ is solved using the energy balance, i.e.,

$$f_{x,aw} = \frac{\dot{m}_r c_{p,r}\left[T_r\left(x = f_{x,aw}L_x\right) - T_{r,1}\right]}{\left[\dot{m}_a \bar{c}_{p,a}\left(T_{a,1} - \bar{T}_{a,fw}\right) + \dot{m}_a \Delta h_{fg}\left(\omega_{a,1} - \bar{\omega}_{a,fw}\right)\right]} \tag{36}$$

Finally, the overall energy balance between the air and refrigerant over the entire tube must be satisfied and is used to compute refrigerant enthalpy at the exit of the tube.
The heat transfer of the Case (c) can be evaluated using the same procedures described above. The additional complication involved in this case is that the fraction of the partially wetted region $f_{x,pw}$ needs to be determined as well. At the position $x = (f_{x,fw} + f_{x,pw})L_x$, the onset location of the wet surface is $f_{y,ow}(x) = 1$. It should be pointed out that the heat transfer of the fully dry region should be computed using the equations in Section 3.1 instead of using the average state method for the fully and partially wet surfaces described in Section 3.2. Finally, the average state of the air leaving the tube is

$$\begin{aligned}
\bar{T}_{a,2} &= \frac{f_{x,fw}T_a\left(0, L_y\right)}{2} + \frac{\left(f_{x,fw} + f_{x,pw}\right)T_a\left(f_{x,fw}L_x, L_y\right)}{2} + \frac{f_{x,pw}T_a\left(f_{x,fw}L_x + f_{x,pw}L_x, L_y\right)}{2} + f_{x,fd}\bar{T}_{a,fd} \\
\bar{\omega}_{a,2} &= \frac{f_{x,fw}\omega_a\left(0, L_y\right)}{2} + \frac{\left(f_{x,fw} + f_{x,pw}\right)\omega_a\left(f_{x,fw}L_x, L_y\right)}{2} + \frac{f_{x,pw}\omega_{a,1}}{2} + f_{x,fd}\omega_{a,1}
\end{aligned} \tag{37}$$

It is worthwhile to mention that when both two-phase and vapor-phase refrigerant exist, the tube will be divided into two portions, i.e., the two-phase portion and vapor phase portion and each of them is evaluated separately. The location of the phase transition point is iterated such that refrigerant enthalpy at the transition point is equal to the saturated vapor enthalpy at the local refrigerant pressure.

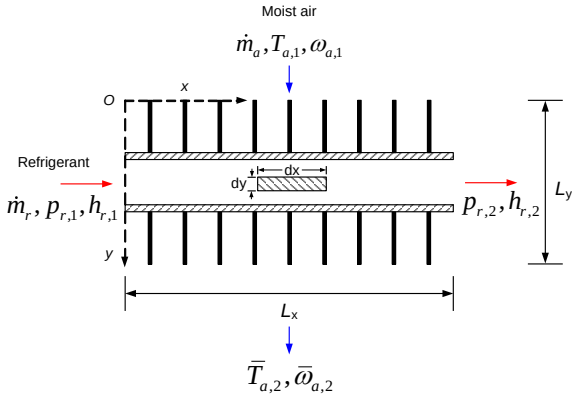

Fig. 4 Schematic of air-to-refrigerant cross-flow

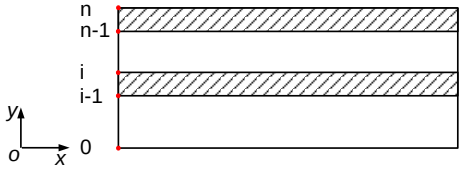

Fig 5. Discretization along the *y* direction

3.4 Model Algorithm

The algorithm of the proposed heat exchanger model is depicted in Fig. 8. Outside the module of tube-by-tube analysis, there are three higher level nested iteration loops. The innermost iteration loop is to compute refrigerant flow distribution for all the circuitries. The next iteration loop uses the successive substitution approach to compute the air state entering each tube. The outermost iteration loop is to compute the air flow distribution for all the face tubes. The innermost and outermost iteration loops involve solving a large-scale system of non-linear pressure drop equalization equations. In order to improve the computational efficiency, these non-linear pressure drop equalization

equations are linearized and solved by a method which is similar to the approach used to solve air flow redistribution due to non-uniform frost growth (Qiao, 2014).

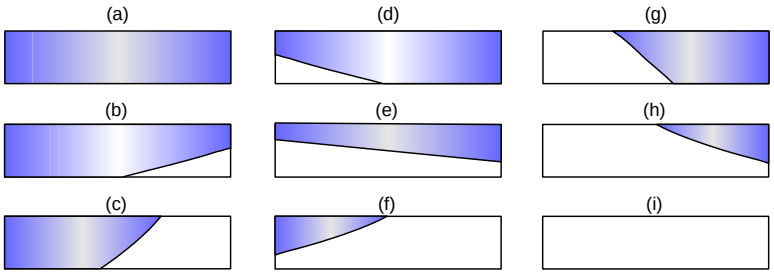

Fig. 6 Possible coil surface conditions: (a) fully wet; (b) fully wet & partially wet; (c) fully wet, partially wet & dry; (d) partially wet & fully wet; (e) partially wet; (f) partially wet & dry; (g) dry, partially wet & fully wet; (h) dry & partially wet; (i) fully dry

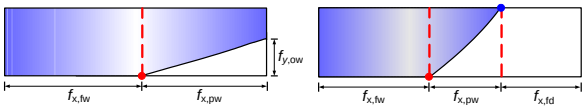

Fig. 7 Surface regions for Case (b) and (c)

4. MODEL VALIDATION

The proposed model was validated using the experimental data reported by McQuinston (1978). The air side heat transfer coefficient in the simulation was calculated using the correlation developed by Wang et al. (2000), and the water side heat transfer coefficient is computed with the Dittus–Boelter correlation (1985). Fig. 9 shows the comparison of the predicted heat load with the measured heat load of the five coils under both dry and wet surface conditions. An overall agreement of 6% is found between the simulation results and the experimental data.

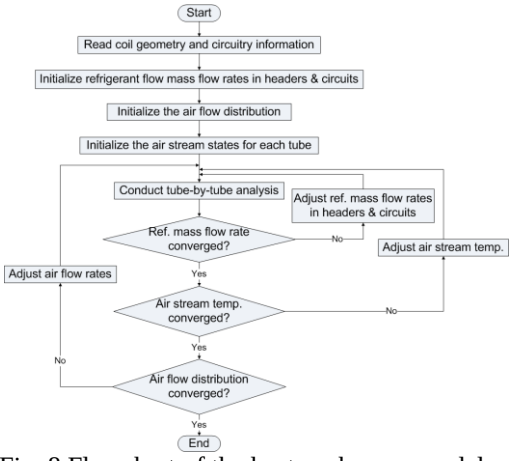

Fig. 8 Flowchart of the heat exchanger model

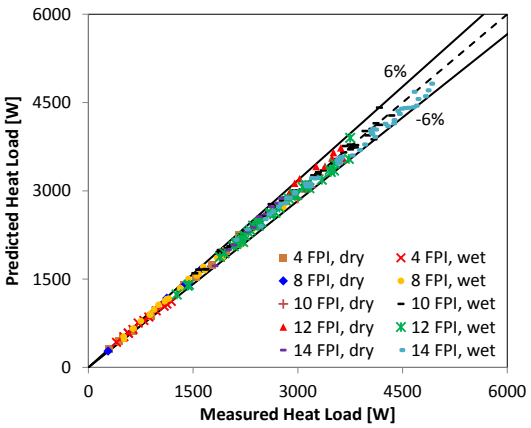

Fig. 9 Model validation against McQuinston (1978)

5. CONCLUSIONS

A new first-principles model has been developed to evaluate the thermal performance of air-to-refrigerant finned-tube heat exchangers under cooling and dehumidifying conditions. The salient features of the model are summarized as follows:

(1) The tube-by-tube approach is employed to allow for the simulation of arbitrary tube circuitries.
(2) Rigorous analysis is embedded in the model to account for fully dry, fully wet and partially wet surface conditions.
(3) Refrigerant phase transition is taken into account.

(4) A novel approach is developed to analyze the air-side simultaneous heat and mass transfer. This new approach allows the Lewis number to deviate from unity. By approximating the saturated air humidity ratio as a cubic function of temperature, the model accuracy can be significantly improved over extant models.
(5) Model validation against experimental data in the literature shows favorable agreement.

NOMENCLATURE

Symbols		***Subscripts***	
A	area	a	air
c_p	specific heat	D	dry condition
f	fraction	dp	dew point
h	enthalpy	f	liquid
L	length	fd	fully dry
Le	Lewis number	fg	liquid to vapor
$\dot{m}$	mass flow rate	fw	fully wet
NTU	number of transfer units	g	vapor
Q	heat transfer rate	m	metal
R	thermal resistance	o	external
T	temperature	pw	partially wet
U	overall heat transfer coefficient	r	refrigerant
ω	humidity ratio	s	saturated
ϕ	surface area ratio	t	temperature
α_m	mass transfer coefficient	w	wall
α_c	heat transfer coefficient	wo	wet surface onset
		W	wet condition

REFERENCES

ARI Standard 410, 2001. Forced-circulation air-cooling and air-heating coils.

Braun, J.E., Klein, S.A., Mitchell, J.W., 1989. Effectiveness models for cooling towers and cooling coils. *ASHRAE Trans*. 95(2), 164-174.

Dittus, F.W., and Boelter, L.M.K., 1985. Heat transfer in automobile radiators of the tubular type. *Int. Commun. Heat Mass* 12 (1), 3-22.

Domanski, P., and Didion. D., 1983. Computer modeling of the vapor compression cycle with constant flow area expansion device. Building Science Series 155.

EI-Din, M.M.S., 1998. Performance analysis of partially-wet fin assembly. *Appl. Therm. Eng.* 18 (5), 337-349.

Lee, J. and Domanski, P.A., 1997. Impact of air and refrigerant maldistributions on the performance of finned-tube evaporators with R-22 and R-407C. Report DOE/CE/23810-81 for ARI, National Institute of Standards and Technology, Gaithersburg, MD.

Jiang, H., Aute. V., Radermacher, R., 2006. CoilDesigner: a general purpose simulation and design tool for air-to-refrigerant heat exchangers. *Int. J. Refrigeration* 29, 601-610.

Liang, S.Y., Wong, T.N., Nathan, G.K., 2001. Numerical and experimental studies of refrigerant circuitry of evaporator coils. *Int. J. Refrigeration* 24, 823 - 833.

McQuiston, F., 1978. Heat, mass and momentum transfer data for five plate-fin-tube heat transfer surfaces, *ASHRAE Trans.* 84, 266–293.

Qiao, H., 2014. Transient modeling of two-stage and variable refrigerant flow vapor compression systems with frosting and defrosting. Ph.D. Thesis, Unversity of Maryland College Park.

Rosario, L. and Rahman, M.M., 1999. Analysis of heat transfer in a partially wet radial fin assembly during Dehumidification. *Int. J. Heat Fluid Flow* 20, 642-648.

Threlkeld, J. L., 1970. Thermal Environmental Engineering. Prentice Hall, Englewood Cliffs, New Jearsy.

Wang, C.C., Chi, K.Y., Chang, C.J., 2000. Heat transfer and friction characteristics of plain fin-and-tube heat exchangers, part II: Correlation. *Int. J. Heat Mass Tran.* 43, 2693-2700.